

July 1998 • NREL/CP-530-23916

The Influence of Grain Boundary Diffusion on the Electro-Optical Properties of CdTe/CdS Solar Cells

*D.H. Levi, L.M. Woods, D.S. Albin, T.A. Gessert,
R.C. Reedy, and R.K. Ahrenkiel*



Presented at the 2nd World Conference and Exhibition on
Photovoltaic Solar Energy Conversion; 6-10 July 1998; Vienna, Austria

National Renewable Energy Laboratory
1617 Cole Boulevard
Golden, Colorado 80401-3393
A national laboratory of the
U.S. Department of Energy
Managed by the Midwest Research Institute
For the U.S. Department of Energy
Under Contract No. DE-AC36-83CH10093

THE INFLUENCE OF GRAIN BOUNDARY DIFFUSION ON THE ELECTRO-OPTICAL PROPERTIES OF CdTe/CdS SOLAR CELLS

D.H. Levi, L.M. Woods,* D.S. Albin, T.A. Gessert, R.C. Reedy, and R.K. Ahrenkiel
National Renewable Energy Laboratory (NREL)
1617 Cole Blvd., Golden, CO 80401 USA
* Colorado State University, Fort Collins, CO 80523, USA

ABSTRACT: We report on a study of the effects of diffusion of metals through polycrystalline CdTe thin films. The metals Ni, Pd, Cu, Cr, and Te are deposited onto the back surface of 10- μm thick CdTe/CdS device structures using room-temperature evaporation. We found that four out of the five metals produce significant changes in the photoluminescence (PL) of the near-junction CdTe material. These changes are explained in terms of spatial variations of the photoexcited carrier distribution and spatial variations in the sulfur composition of the CdTeS alloy material near the CdTeS interface. The changes in carrier distribution appear to be associated with band bending and electric fields induced by diffusion of the metals to the CdTe/CdS interface. In addition to PL measurements, we have also utilized a technique for detaching the CdTe film from the CdS/TCO/glass superstrate to directly access the front surface of the CdTe absorber layer. We have used secondary ion mass spectroscopy to measure the metal diffusion profiles from this interface.

Keywords: CdTe - 1: Grain Boundary Diffusion - 2: Spectroscopy - 3

1. INTRODUCTION

It is widely recognized that grain boundaries exert significant influence on the electrical and optical properties of polycrystalline semiconductors used in thin-film solar cells. Grain boundaries tend to have a high concentration of lattice defects and impurities. This can make them a dominant factor in the electrical properties of a polycrystalline semiconductor. Diffusion of impurities along grain boundaries in polycrystalline thin-film CdTe/CdS solar cells is likely to be several orders of magnitude faster than diffusion through the bulk.^[1] Rapid diffusion along grain boundaries will have a significant influence on the results of post-deposition processing such as CdCl₂ treatment and back contact application. Thus it is important to further our understanding of diffusion of impurities along grain boundaries and of how such diffusion processes affect the electronic and optical properties of CdTe/CdS solar cells.

2. EXPERIMENTAL CONDITIONS

2.1 Samples

Samples in this study consist of close-spaced sublimated CdTe on 800Å thick chemical-bath deposited CdS on SnO₂ / 7059 glass superstrates. The CdTe thickness is approximately 10 μm with a grain size which varies from approximately 1 μm at the front of the film to approximately 5 μm at the back surface. All samples have undergone a 400° C post-growth vapor-CdCl₂ treatment. Efficiencies for cells fabricated from these films are in the range of 12 - 14%. Evaporation at approximately 300 K is used to deposit 500 Å of the metals Ni, Pd, Cu, Cr, and Te onto the back surface. Half of each sample is then annealed for 30 minutes at 300° C in a flowing helium atmosphere. Ion-beam milling is then used to remove the metal layer from both annealed and unannealed pieces of each sample. Annealed and unannealed pieces are then halved again. One half of each undergoes ion-beam milling to remove 1 μm of CdTe from the back surface of the film. The other half of each of these pairs undergoes a "lift-off" procedure^[2] which separates the film at the

CdTe/CdS interface. Secondary Ion Mass Spectroscopy (SIMS) is then used to measure a depth profile of the metal concentration within the film.

2.2 Photoluminescence

Room-temperature, pulsed-excitation PL spectra are measured at each step of the above process. Typical room-temperature PL measurements on polycrystalline CdTe (px-CdTe) are dominated by recombination at defects because of the high density of defect states relative to the photoexcited carrier density. The PL spectra described in this study are unique in that a cavity-dumped dye laser is used as the excitation source. The laser provides pulses 5 picoseconds in duration at a repetition rate of 1 Mhz. Because of the extremely low duty cycle of the laser, we are able to inject much higher photoexcited carrier densities than are practical with a CW laser. Initial carrier densities immediately after the laser pulse are approximately $4 \times 10^{16} \text{ cm}^{-3}$. At these high-injection conditions, the PL spectra are dominated by band-to-band recombination, which we have verified by studying the density-dependence of the spectra^[3]. Photoexcitation is through the transparent CdS window layer at a wavelength of 600nm. The 1/e penetration depth for this wavelength in CdTe is 0.2 μm . Numerical modeling indicates that over 90% of the photoexcited carriers recombine within 3000 Å of the CdTe/CdS interface, hence the term junction photoluminescence. The measurement is conducted under open circuit conditions. Spectral resolution is 1 nm, which corresponds to approximately 2 meV in the wavelength range of interest.

2.3 Secondary Ion Mass Spectroscopy

The SIMS measurements were carried out using a Cameca IMS-5F instrument. A beam of O₂⁺ purified by a mass filter was used as the source of the primary ions. The impact energy of the primary ion beam was 5.5 keV at a incident angle of 42° from the surface normal. The primary current was 250 nA. An area of 200x200 μm^2 was raster scanned. Positive secondary ions generated from the sample were accelerated normal to its surface and were detected at 4.5 keV. Secondary ions were collected from a 60- μm^2 area in the center of the raster scanned area to

minimize effects from the crater walls. High-mass resolution techniques were utilized in the separation of $^{63}\text{Cu}^+$ from $^{126}\text{Te}^{++}$. In the sample chamber, the working pressure was 2×10^{-10} Torr. Secondary ions were counted by an electron multiplier detector.

3. EXPERIMENTAL RESULTS

3.1 Photoluminescence Results

As discussed above, the conditions of our PL experiment measure band-to-band recombination spectra of an approximately 3000-Å thick layer on the CdTe-side of the CdTe/CdS interface. Fig. 1 illustrates the typical junction PL spectrum measured on NREL polycrystalline CdTe/CdS/TCO and CdTe/TCO device structures. All deposition and treatment conditions are identical for the two films. The only difference is the presence of the CdS layer in one film. The differences in the two spectra are striking. The CdTe/TCO film spectrum consists of a single gaussian peak at the 1.51-eV bandgap energy of CdTe. The CdTe/CdS/TCO film spectrum consists of two peaks that can be fit with a sum of two gaussians. The fitting functions are illustrated by the dashed lines in Fig.1.

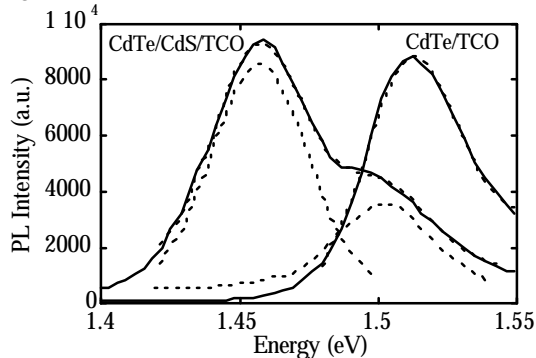


Figure 1: Junction PL spectra for pre-metalization devices illustrating effect of presence of CdS layer. Dashed lines demonstrate Gaussian fits.

The peak energies of the two peaks in the CdTe/CdS/TCO spectrum are 1.501 and 1.457 eV, respectively. The bandgap of a CdTeS alloy initially decreases as sulfur is added to CdTe up to a sulfur concentration of approximately 20%^[4]. We have done a linear fit to the CdTeS alloy bandgap dependence on sulfur concentration for concentrations below 20%, and have come up with a reduction of 4.5 meV in bandgap for each 1% increase in sulfur concentration. We conclude that the two peaks in the CdTeS spectrum are due to regions of alloy with compositions of 2% and 12%, respectively. The 12% composition is consistent with grazing-incidence x-ray diffraction measurements of alloy composition on lift-off samples,^[5] which probe only the first 50 Å of the film. It is not clear at this time why the spectrum displays two distinct peaks rather than a single broad peak spanning the range of bandgap energies from 12% to 0% sulfur. Possible explanations are an electric field-induced segregation of photoexcited carriers, or a CdTeS alloy composition distribution which is bi-modal instead of changing smoothly with distance from the interface

The effects of evaporation of 500 Å of Cr on the back surface of a CdTe/CdS/TCO film are illustrated in Fig. 2. The premetalization spectrum is shown for comparison.

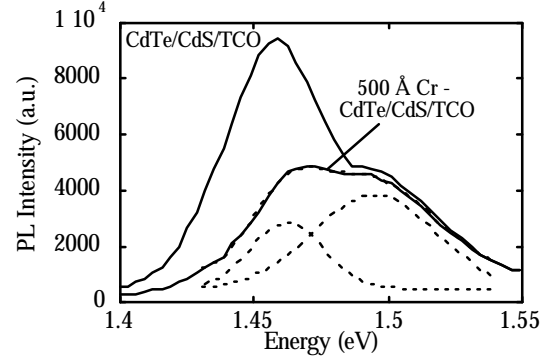


Figure 2: Junction PL spectra for non-metalized and 500 Å Cr sample illustrating the nature of the changes induced in the spectra by metalization.

The spectrum can still be fit with two gaussian peaks, but in this case both peaks have shifted in energy, and the relative intensity ratio between the two peaks has changed significantly. In this case, the peaks are at 1.494 and 1.462 eV. This corresponds to sulfur compositions of 4% and 11%, respectively. Similar changes have been observed with Ni, Pd, and Te. Copper is the only metal that failed to produce significant changes in the junction PL spectrum.

The intensity ratio between low and high energy peaks in the PL spectrum is a useful method for quantifying the degree of perturbation in the spectrum. The value of this ratio for all samples prior to metalization is in the range 2.7 ± 0.2 . After metalization, the ratio is reduced to less than one for some metals. We find that for some of the metals these effects are significantly enhanced by annealing. It is rather surprising that Cu produces little if any effect, as Cu is known to be an effective dopant and a fast diffuser in CdTe^[6].

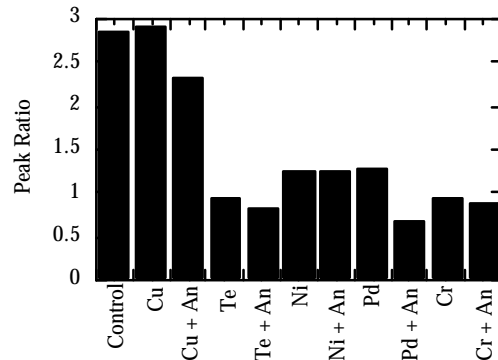


Figure 3: Peak ratio in PL spectrum vs. metalization and annealing. Ratio increases with intensity in lower energy peak.

PL spectra were measured after both the shallow and deep ion-beam milling of the back surface of metalized and metalized-and-annealed samples. The spectra reverted back to their pre-annealed character with shallow milling for all but the annealed Cr and annealed Pd samples. The deep ion-beam milling step reverted the PL spectra for the latter two samples. These results appear to suggest that the metalization-induced changes in the junction PL spectra are due to a back-surface field (BSF) effect.

To investigate the BSF hypothesis, we have measured junction PL under bias on a completed device. We find that the shape of the spectrum is unchanged for short-

circuit, open-circuit, and 10-V reverse-bias conditions. If the observed changes in the PL spectra with metalization were due to a BSF effect, we would expect application of a 10 V-bias to produce large changes in the shape of the PL spectrum.

We have also used the numerical device modeling program SimWindows™ to simulate the effects of a large BSF on the electric fields and photoexcited carrier distributions at the CdTe/CdS interface. The results show no changes at all in fields or carrier distributions near the junction unless the bulk doping in the CdTe absorber layer is reduced to 10^{13} cm^{-3} or lower. Capacitance measurements have indicated that the carrier density in the p-type CdTe absorber layer of NREL CdTe/CdS devices is in the range of 10^{15} cm^{-3} . We conclude that it is not likely that the changes in junction PL with metalization are caused by a BSF.

3.2 SIMS Results

SIMS depth profiles on lift-off samples have been successfully carried out on the Cr, Pd, and Cu samples. For the Cu sample, Cu penetrates approximately $1 \mu\text{m}$ into the film prior to annealing. After annealing Cu is distributed throughout the film at a concentration between 0.01 and 0.1 %. This is an extremely high concentration, which verges on a Cu:CdTe alloy rather than a dopant or impurity. SIMS has a rather low sensitivity for Pd. Prior to annealing, Pd is detected only near the back surface of the device. After annealing, there is a significant SIMS-Pd signal throughout the device. We have been unable to quantify the concentration of Pd because of a lack of calibrated sensitivity factors for Pd in CdTe or HgCdTe.

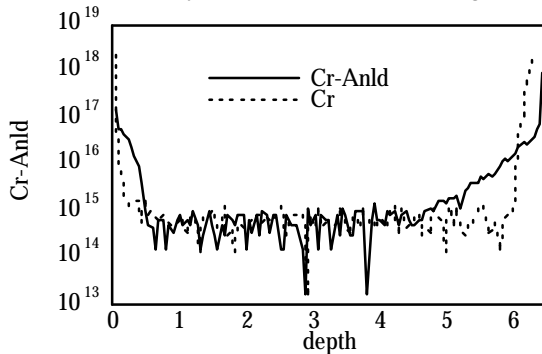


Figure 4: SIMS profile of Cr concentration in sample before and after annealing.

Fig. 4 presents the Cr diffusion profiles. Prior to annealing, the Cr signal is above background only near the front and back interfaces. The nonzero Cr signal at the front interface is inconclusive, as this could be due to environmental contamination. After annealing, Cr penetrates almost $2 \mu\text{m}$ into the back of the film, and roughly $0.5 \mu\text{m}$ into the front of the film. We note that the measured Cr distribution at the front of the film is nonhomogeneous, most likely caused by inhomogeneity in the film-diffusion properties. The SIMS concentration calibration was estimated due to the lack of CdTe SIMS standards. Relative sensitivity factors (RSFs) were calculated for Cu and Cr based on published HgCdTe RSFs^[7].

Because SIMS measures many grains and grain boundaries at once we must also take into account the volume of grain boundaries relative to the total volume. This ratio will depend on the grain size and the width of the

grain boundaries. For a rough estimate we have assumed rectangular grains with planar grain boundaries. For the films used in this study the grains are approximately $1 \mu\text{m}$ in diameter and we estimate 10 \AA thick grain boundaries. In this case the grain boundaries make up 0.2 % of the total film volume. If we make the simplifying assumption that the metals are completely contained within the 10 \AA thick grain boundaries this implies that concentrations measured by SIMS are a factor of 5×10^2 lower than the concentration within the grain boundary. This means an impurity can be present in the grain boundaries at relatively high doping levels (e.g. 10^{18} cm^{-3}) and still be below the SIMS baseline.

4. DISCUSSION

4.1 Model for Junction Photoluminescence

The key to understanding the changes observed in the junction PL spectra is the relationship between the spatial extent of sulfur diffusion into the CdTe absorber layer and the spatial distribution of photoexcited carriers under our experimental conditions. Figure 5 illustrates this relationship. This double-y plot shows a model calculation^[8] of the spatial extent of recombination under the experimental conditions described in section 2. The radiative recombination distribution is shown by dashed lines for two different surface recombination velocities (SRV). Superimposed is a SIMS profile of the sulfur distribution as a function of distance from the CdTe/CdS interface. The CdTeS alloy bandgap will shift 4.5 meV for each 1% change in the sulfur composition of the alloy. Thus, a spatial shift in the recombination distribution will produce a shift in the peak energy of the junction PL.

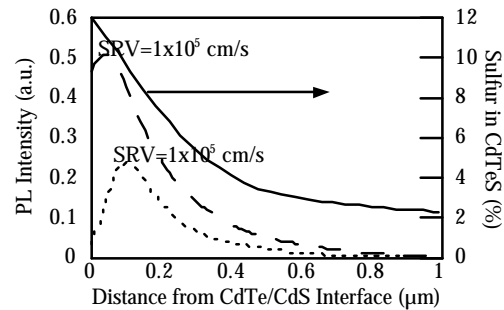


Figure 5: Spatial distribution of recombination vs. sulfur alloy composition in CdTe layer. Dashed lines show recombination for two different values of SRV.

In the model calculation of Fig. 5 we have used variations in SRV to produce changes in the recombination distribution. Band-bending, electric fields, and changes in doping can produce similar or more complex redistributions of the carrier and recombination distributions. It should also be noted that the SIMS profile of sulfur distribution is an average over many grains and grain boundaries. It is likely that the actual alloy composition has abrupt local variations which are averaged out by the "macroscopic" SIMS measurement. Such abrupt variations could produce the two-peaked structure observed in junction PL measurements.

4.2 Grain-Boundary Diffusion

Grain-boundary (GB) diffusion processes in thin films can be significantly different than GB diffusion in bulk material. Grain-boundary diffusion lengths can equal or exceed the film thickness. In this case the back surface of the film can significantly affect the diffusion profiles. Gilmer and Farrell^[1] have studied the problem of GB diffusion in thin films for various boundary conditions. Figure 6 presents their numerical modeling results for conditions where GB diffusion is coupled with bulk diffusion. The film thickness is D , and there is an infinite reservoir of diffusant at the surface labeled 0. Two boundary conditions are considered; 1) the surface at D is a barrier for further diffusion, or 2) there is rapid diffusion parallel to the surface at D .

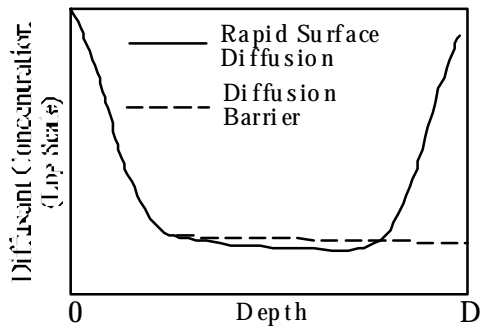


Figure 6: Numerical modeling results for grain boundary diffusion showing the effect of rapid surface diffusion at the buried interface D .

The latter case is the solid line in Fig. 6. Impurity atoms diffuse through the grain boundaries and spread out at the surface D . This surface then acts as a new source of impurities for diffusion back into the bulk. The profile for case number two is quite similar to the SIMS profile for the annealed Cr sample as shown in Fig. 4. Note that the two figures are right-to-left mirror images of each other.

The model of Fig. 6 together with the SIMS profile of Fig. 4 provides a possible scenario for the distribution of metals under the conditions in this study. If GB diffusion is significantly faster than bulk diffusion the metals will be located primarily within in the GB's and at the front surface. The concentrations of metallic impurities in the GB's will be roughly 500 times higher than the values measured by SIMS. For the SIMS results of Fig.4 this corresponds to an upper limit on concentration for GB's in the middle of the film of approximately $5 \times 10^{17} \text{ cm}^{-3}$, and somewhere between 1×10^{17} and $5 \times 10^{19} \text{ cm}^{-3}$ at the CdTe/CdS interface. If the metallic impurities are active as dopants these concentrations would make the GB's channels of high conductivity within the relatively low-doped p-type CdTe matrix.

4.3 Implications for PL Spectra

It was noted in section 3.1 that removal of the metallic layer from the back surface using ion-beam milling caused the junction PL spectrum to revert to its pre-metalization character. The two exceptions, annealed Pd and annealed Cr, did not revert until an additional $1 \mu\text{m}$ of CdTe was removed. SIMS profiles revealed that these two metals penetrated several microns at the back surface with annealing.

We are lead to postulate the following model of the effect of GB diffusion on junction PL. From electrostatics we know that a metal will not support an electric field, all

of the metal remains at a single electrical potential. When the metallic layer is present on the back surface it provides a "grounding layer" which connects all of the grain boundaries, and through the GB's, the front surface. This effect produces the band bending at the front surface which perturbs the junction PL spectra. When the metallic layer is removed from the back surface the GB's are no longer connected together and essentially "float" at the potential of the bulk material surrounding them. This eliminates the band bending at the front surface and the PL spectrum reverts to its pre-metalization character. The samples with annealed Cr and Pd required further ion-beam milling because of the deep penetration of the metals at the back surface. Copper failed to produce a shift in the PL spectrum because it is highly mobile in the bulk of CdTe and dopes grains and GB's equally. This is consistent with the high Cu concentrations measured by SIMS.

CONCLUSIONS

Device modeling and bias-dependent PL measurements imply that the changes in junction PL spectra produced by metal deposition are not due to a back-surface field effect. SIMS depth profiles and theoretical modeling of diffusion in polycrystalline thin films indicate that metals deposited on the back surface rapidly diffuse along the grain boundaries and may accumulate at the CdTe/CdS interface. Highly-doped GB's act as conduction pathways to connect the front and back surfaces, maintaining both surfaces at the same potential. These perturbations will alter the spatial distribution of radiative recombination, producing the observed changes in the junction PL spectra. The exact nature of the shifts in peak energy and relative intensity is difficult to explain without detailed knowledge of the spatial composition of the CdTeS alloy near the interface. The two-peak structure of the junction-PL implies some type of metastable miscibility gap in the alloy composition not predicted by equilibrium phase diagrams.

ACKNOWLEDGEMENTS

The authors wish to thank Anna Duda for extensive assistance with metals deposition. We also thank Falah Hasoon, Alice Mason, and David King for evaporation of copper, EPMA and XPS, respectively. This project was funded by the U.S. Department of Energy under contract DE-AC36-83CH10093.

REFERENCES

- [1] I. Kaur et.al. in Fundamentals of Grain and Interphase Boundary Diffusion, p.2, (J. Wiley and Sons, Chichester), 1995.
- [2] see Woods, et.al. in these proceedings.
- [3] D.H. Levi, et.al, Proceedings of the 26th IEEE PVSC, Anaheim, CA, 1997, p351.
- [4] ibid, [3].
- [5] D. Albin, et.al., Fall 1997 Materials Research Society Symposium G, Boston, MA."
- [6] H.C. Chou, et.al., J. Elect. Mat., **25**, p.1093,(1996).
- [7] R. G. Wilson, et.al., Secondary Ion Mass Spectrometry: A Practical Handbook for Depth Profiling and Bulk Impurity Analysis (Wiley, New York, 1987)

[⁸] based on analytical solution in J. Vaitkus, Phys. Stat. Sol., **34**, p.769 (1976).

[⁹] G.H. Gilmer and H.H. Farrell, J. Appl. Phys. **47** (1976), p.4373.